Supplementary Information

One-Step growth of 3D cross-linked $NiCo_2S_4$ nanosheet and $CoNi_2S_4$ nanorod arrays on carbon paper as anodes for high-performance lithium ion battery

Weiwei Yang,[a] Liang Chen,[b] Jie Yang,[b] Chun Fang,[a] Xiang Zhang,[a] Zhiling Chen,[a] Lin Huang,[a] Jianguo Liu,[a,b,c*] Yong Zhou,[b] and Zhigang Zou [a,b**]

[a] *National Laboratory of Solid State Microstructures, College of Engineering and Applied Sciences, and Collaborative Innovation Center of Advanced Microstructures, Nanjing University, 22 Hankou Road, Nanjing 210093, China.*

[b] *Jiangsu Key Laboratory for Nano Technology, Department of Physics, Nanjing University, 22 Hankou Road, Nanjing 210093, China.*

[c] *Kunshan Sunlaite New Energy Co., Ltd., Kunshan, 1699# South Zuchongzhi Road, Suzhou, 215347, China.*

Experimental Section

Preparation of $CoNi_2S_4$ and $NiCo_2S_4$.

Before using it, commercial carbon paper (CP) was ultrasonically cleaned in ethanol and deionized water for 30 min respectively. In a typical synthesis, 2.5 mmol $Co(CH_3COO)_2\ 4{\cdot}H_2O$, 1.25 mmol $Ni(CH_3COO)_2\ 4{\cdot}H_2O$ and 6 mmol thiourea (CN_2H_4S) were mixed for 30 min to form a puce solution with 30 ml deionized water and 10 ml ammonia hydroxide (~ 28%) as solvent at 25 ^oC. After, the mixture of puce solution and cleaned carbon paper (CP) were transferred into a Teflon-lined stainless steel autoclave of 100 mL inner volume, which was subsequently heated at 160 °C for 10 h. After the hydrothermal reaction, the CP was taken out from above mixed solution at room temperature and further cleaned by ultrasonication for 5 min to remove the attached products on the surface. After washed with deionized water and ethanol for several times, the 3D cross-linked $NiCo_2S_4$ nanosheet arrays ($NiCo_2S_4$ NSAs-CP) were obtained. In order to improve the crystallinity, the $NiCo_2S_4$ NSAs-CP were annealed under N_2 atmosphere at 350 ^oC for 2 h. Meanwhile, 3D $CoNi_2S_4$ nanobelt arrays ($CoNi_2S_4$ NRAs-CP) also can be obtained with 1.25 mmol $Co(CH_3COO)_2\ 4{\cdot}H_2O$ and 2.5 mmol $Ni(CH_3COO)_2\ 4{\cdot}H_2O$ while other condition not changed.

Characterizations

X-ray powder diffraction patterns were performed on a Philips X-ray diffractometer (APD 3520) equipped with Cu Kα radiation. The morphologies observations (SEM) and composition analysis (energy-dispersive X-ray spectroscopy, EDX) of the samples were carried out on S-4800 scanning electron microscopy (SEM) operating at 5 kV. The transmission electron microscopy (TEM) and high-resolution transmission electron microscopy (HR-TEM) images were collected by JEM 200CX TEM instrument.

Electrochemical measurement

The 3D $CoNi_2S_4$ NRAs-CP and cross-linked $NiCo_2S_4$ NSAs-CP were directly used as working electrodes without adding any other assist materials. The loading weight of the $CoNi_2S_4$ NRAs-CP and $NiCo_2S_4$ NSAs-CP (the active material) were about 2 ± 0.3 mg (1.300 ± 0.195 mg·cm^{-2}) and CP was 12.23 mg (7.949 mg ·cm^{-2}). In addition, pure CP was also used as cathode to compare with $CoNi_2S_4$ NRAs-CP and $NiCo_2S_4$ NSAs-CP and reference. The electrochemical performance were evaluated with a standard CR2032 coin cell using lithium foils as the anode, microporous polypropylene separator (Celgard 2400) as the separator, and electrolyte solution was made of 1 M $LiPF_6$ in ethylene carbonate (EC) and diethyl carbonate (DEC) (1/1, in volume). The coin-type cells were assembled in an argon-filled glove box, where both moisture and oxygen levels were less than 1 ppm. Galvanostatic charge-discharge cycles were tested by LAND CT 2001A multi-channel. Cyclic voltammeter (CV) was conducted by using Princeton Applied Research PARSTAT 2273 at scanning rate of 0.1 mV·s^{-1} between 0.01–3.0 V.

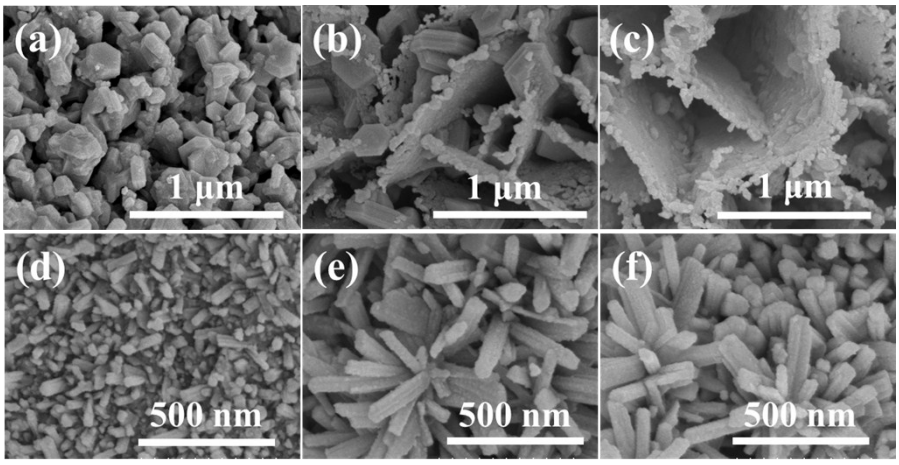

Fig. S1 Typical SEM images of $NiCo_2S_4$ NSAs-CP synthesized for 2.5 h (a), 5 h(b) ,7.5 h (c) and

$CoNi_2S_4$ NRAs-CP synthesized for 2.5 h (d), 5 h (e) ,7.5 h (f)

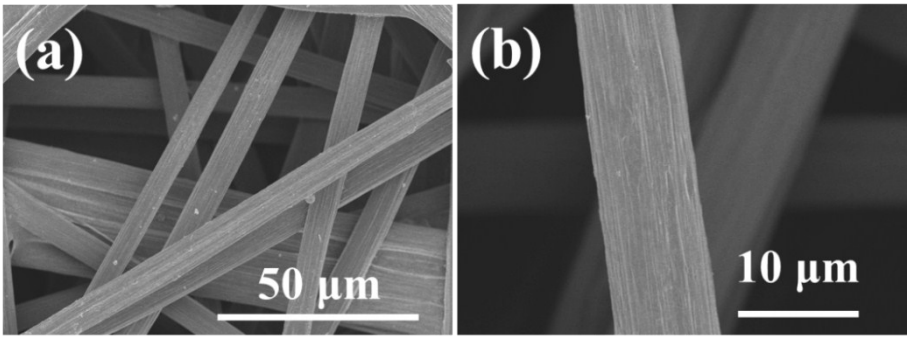

Fig. S2 Typical low (a) and magnified (b) SEM images of pure CP.

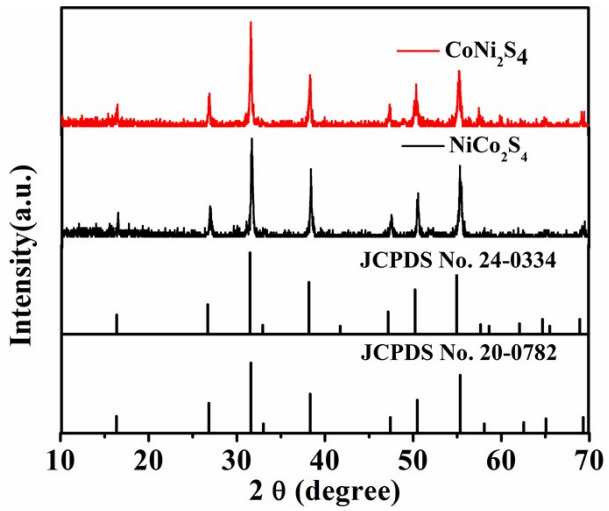

Fig. S3 XRD spectrum of $NiCo_2S_4$ and $NiCo_2S_4$ ultrasonic treatment from CP.

The phase structure of $CoNi_2S_4$ and $NiCo_2S_4$ was characterized by X-ray diffraction (XRD) as shown in Fig. S3. The crystalline phase of the as-prepared samples can be identified as $CoNi_2S_4$ (JCPDS No. 24-0334) and $NiCo_2S_4$ (JCPDS No. 20-0782) with very similar cubic structures. Besides, no other characteristic peaks can be observed, suggesting that both samples have no other impure phases.

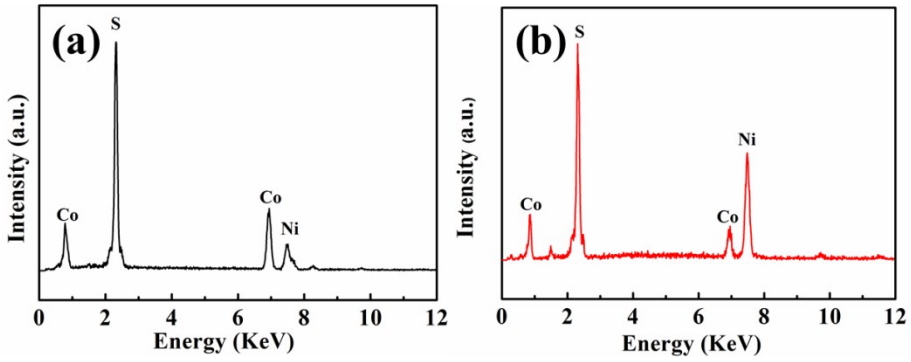

Fig. S4 EDX of $NiCo_2S_4$-CP (a) and $NiCo_2S_4$-CP (b).

The samples were further characterized by energy-dispersive X-ray spectroscopy (EDX, Fig. S4), which indicates that the Ni/Co atomic ratios of $CoNi_2S_4$ and $NiCo_2S_4$ are 1.85 : 1 and 1: 2.08, respectively. The reason for the relatively small amount for the Ni atomic ratios could be ascribed to bits of Ni^{2+} ions being reduced to metallic nickel.

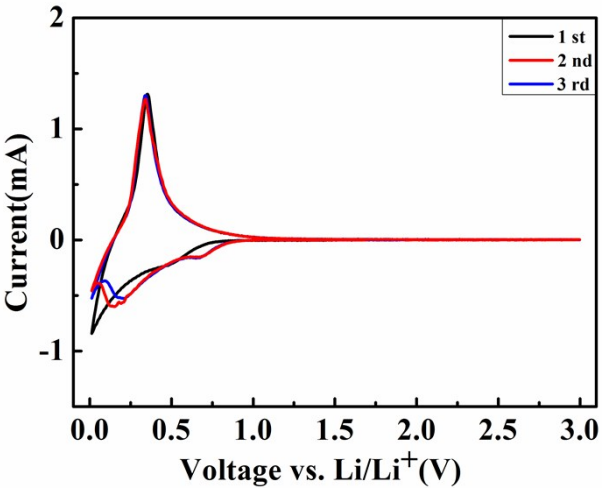

Fig. S5 CV curves of pure CP at the scan rate of 0.1 mV s^{-1} between 0.01 and 3 V.

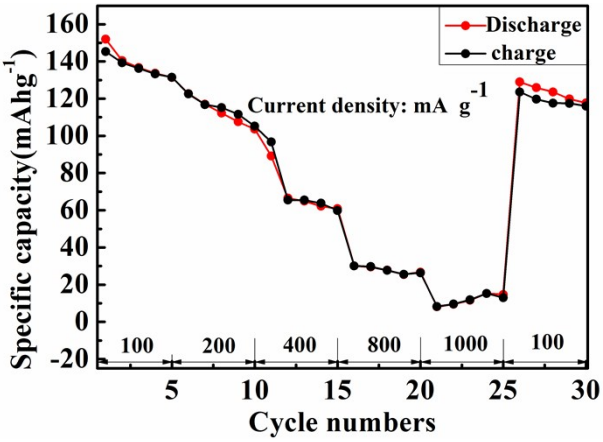

Fig. S6 Rate performance of pure CP electrode at 100, 200, 400, 800 and 1000 mA g^{-1}.

The current collector of CP will insert an amount of Li during the discharge process and finally increase the specific discharge capacity. The specific discharge capacity of the pure CP electrode at 100, 200, 400, 800 and 1000 mA g^{-1} are shown in Fig. S6.

Table S7 Rate performance of synthesized $NiCo_2S_4$ NRAs-CP and $CoNi_2S_4$ NRAs-CP compared with previous published studies on binary or ternary Co/Ni based sulfides.

Species (mA h g^{-1})	Current density (mA g^{-1})					Reference
	100	200/250	400/500	800	1000	
$NiCo_2S_4$ NSA/carbon cloth	1950	/	1220	/	1030	[1]
$NiCo_2S_4$ nanorod	~1200	~1100	~900	/	~800	[2]
NiS	~650	~550	~500	/	~500	[3]
Ni_3S_2 nanotube array	495	466	453	/	418	[4]
CoS_2/G	~650	~550	~450	~400	/	[5]
Co_9S_8	904	810	751	/	699	[6]
Our $NiCo_2S_4$ NSAs-CP	2363.3	2107.8	1712.4	1242.1	707.7	/
Our $CoNi_2S_4$ NRAs-CP	1979.3	1728.8	1418.6	897.8	465.2	/

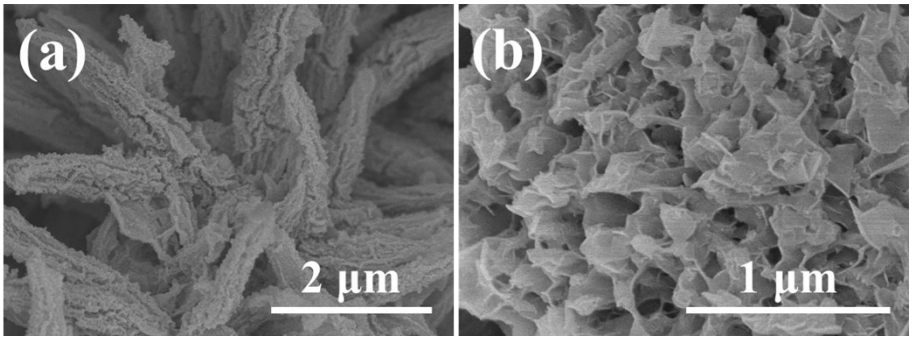

Fig. S8 Typical SEM images of $NiCo_2S_4$ NSAs-CP (a) and $CoNi_2S_4$ NRAs-CP (b).

Table S9 The specific discharge capacity of $NiCo_2S_4$ NRAs-CP, $CoNi_2S_4$ NRAs-CP, CP, $NiCo_2S_4$ NRAs and $CoNi_2S_4$ NRAs.

Species (mA h g^{-1})	Current density (mA g^{-1})				
	100	200	400	800	1000
Total $NiCo_2S_4$ NSAs-CP	2363.3	2107.8	1712.4	1242.1	707.7
Total $CoNi_2S_4$ NRAs-CP	1979.3	1728.8	1418.6	897.8	465.2
CP	152.0.	122.7	89.2	30.1	8.1
Actual $NiCo_2S_4$ NSAs-CP	1433.8	1357.5	1166.9	1058.0	695.4
Actual $CoNi_2S_4$ NRAs-CP	1049.8	978.5	873.1	713.7	415.7

Notes and references

1. R. J. Zou, Z. Y. Zhang, M. F. Yuen, M. L. Sun, J. Q. Hu, C.-S Lee and W. J. Zhang, *NPG Asia Mater.*, 2015, **7**, 1.
2. Y. Luo, M.-S. Balogun, W. T. Qiu, R. R. Zhao, P. Liu and Y. X. Tong, *Chem. Commun.*, 2015, **51**, 13016.
3. H. Geng, S. F. Kong and Y. Wang, *J. Mater. Chem. A.*, 2014, **2**, 15152.
4. D. Li, X. W. Li, X. Y. Hou, X. L. Sun, B. L. Liu and D. Y He, *Chem. Commun.*, 2014, **50**, 9361.
5. J. Xie, S. Y. Liu, G. S. Cao, T. J. Zhu and X. B. Zhao, *Nano Energy* 2013, **2**, 49.
6. Y. L. Zhou, D. Yan, H. Y. Xu, S. Liu, J. Yang and Y. T. Qian, *Nanoscale*, 2015, **7**, 3520.